Materials Advances

ROYAL SOCIETY OF CHEMISTRY

PAPER

View Article Online
View Journal | View Issue

Cite this: *Mater. Adv.*, 2025, **6**, 9568

Design and synthesis of thermally robust pyrazine–tetrazole hybrids as high-nitrogen energetic materials

Jatinder Singh, [a] Richard J. Staples [b] and Jean'ne M. Shreeve *[a]

The development of advanced heat-resistant energetic materials for extreme environments demands molecular frameworks that combine high decomposition temperatures, strong detonation performance, and synthetic accessibility. In this study, nitrogen-rich pyrazine–tetrazole hybrids designed to achieve this balance are introduced. Pyrazine cores, functionalized with amine-tetrazole units, promote dense molecular packing owing to hydrogen-bond networks, resulting in enhanced thermal stability. Thermal analysis discovered decomposition onset temperatures of 305 °C (compound **2**) and 320 °C (compound **5**), values surpassing TNT (295 °C) and approaching HNS benchmarks (318 °C). Calculated detonation velocities (7383 and 7278 m s^{-1}) and detonation pressures (18.8 and 18.2 GPa) highlight their energetic efficiency while maintaining reduced sensitivity compared to conventional polynitro systems. Importantly, the synthetic approach employs facile precursor transformations, underscoring scalability. Together, these findings demonstrate a rational pathway toward nitrogen-rich heterocycles that function as structurally robust, thermally stable high-energy-density materials (HEDMs). This work provides new insights into molecular innovation and expands the design landscape for insensitive explosives, extending the operational limits of energetic systems in aerospace, defense, and industrial applications.

Received 2nd October 2025,
Accepted 27th October 2025

DOI: 10.1039/d5ma01131k

rsc.li/materials-advances

1. Introduction

The synthesis of energetic compounds is a pivotal aspect of applied materials research, requiring a delicate balance between achieving high performance and ensuring feasibility in terms of manufacturability, scalability, and safety.[1–5] While some energetic compounds require complex multi-step synthetic routes with harsh conditions, others can be synthesized through relatively straightforward procedures, utilizing readily available precursors and conventional reaction methodologies.[6–10] The ease of synthesis of an energetic material is often a determining factor in its widespread adoption, particularly in military, aerospace, and industrial applications where cost-effectiveness and production efficiency are paramount.[11–15] Addressing these challenges requires molecular innovations in scaffold design that precisely tune heats of formation, density, and intermolecular interactions to maximize energetic performance while minimizing sensitivity.[16–20]

Conventional energetic materials, while highly effective within controlled environments, often suffer from thermal degradation when exposed to elevated temperatures.[21] This sensitivity poses significant challenges in various applications, such as deep-space propulsion, hypersonic weapons, and high-temperature industrial operations, where prolonged thermal exposure can lead to autoignition and detonation failure.[22–24] Heat-resistant energetic materials are designed with enhanced thermal stability through strategic molecular modifications, high-entropy energetic compounds, and advanced polymeric binders capable of withstanding extreme heat without compromising detonation efficiency (Fig. 1A).[25–33] The future of heat-resistant explosives lies in the convergence of molecular design, and energetic architectures, pushing the boundaries of performance in extreme operational environments (Fig. 1B).[34–40]

Among nitrogen-rich heterocycles, pyrazine derivatives provide a versatile platform for designing thermally robust energetic materials.[41,42] Notable examples include ANPZ and LLM-115, which exhibit exceptionally high decomposition temperatures along with low sensitivity to impact and friction.[43] The electron-deficient nature of the pyrazine ring allows for the facile incorporation of substituents such as nitro, amino or cyano groups, which can subsequently be transformed into high-nitrogen functionalities. Furthermore, the symmetric arrangement of substituents on the pyrazine core promotes

[a] *Department of Chemistry, University of Idaho, Moscow, ID 83844-2343, USA. E-mail: jshreeve@uidaho.edu*
[b] *Department of Chemistry, Michigan State University, East Lansing, Michigan 48824, USA*

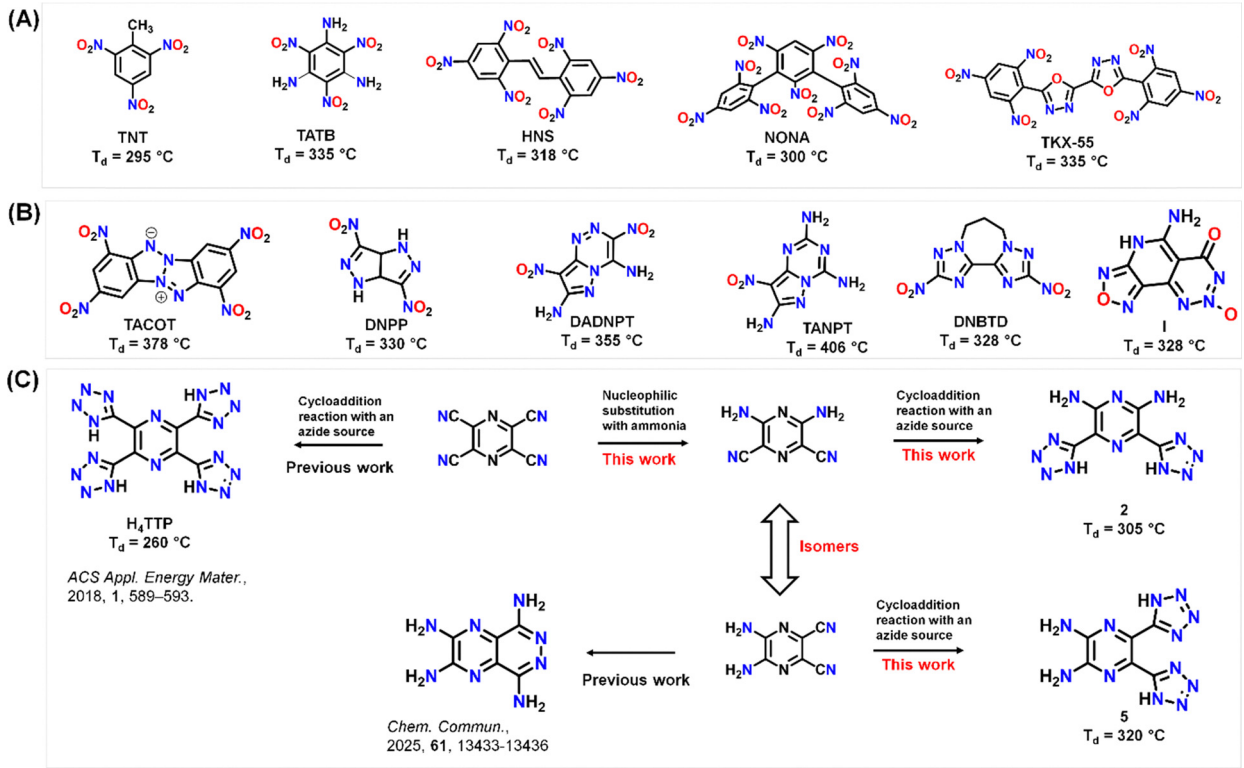

Fig. 1 (A) Phenyl-containing heat resistance energetic materials. (B) Fused-ring based heat resistance energetic materials. (C) This work.

dense molecular packing and extensive hydrogen-bonding networks, both of which enhance thermal stability. Recent studies have shown that pyrazine–tetrazole hybrids can achieve high enthalpies of formation while maintaining reduced sensitivity compared to conventional polynitro systems (Fig. 1C).[44,45] This dual advantage of stability and energy density underscores the promise of pyrazine-based frameworks as attractive scaffolds for next-generation heat-resistant energetic materials.

2. Results and discussion

2.1. Synthesis

Pyrazine-2,3,5,6-tetracarbonitrile (**P2**) was synthesized from commercially available diaminomaleonitrile (**P1**) following a previously reported method.[44] This intermediate was then treated with ammonia in methanol at ambient temperature leading to the formation of 3,5-diaminopyrazine-2,6-dicarbonitrile (**1**) in a nearly quantitative yield (Scheme 1).

Subsequently, compound **1** was reacted with sodium azide in dimethyl sulfoxide (DMSO) at 130 °C, facilitating the conversion into 3,5-di(1*H*-tetrazol-5-yl)pyrazine-2,6-diamine (**2**) through a tetrazole ring formation process. The synthesis of the corresponding 2,3-isomer followed a distinct route, starting from commercially available 5,6-dichloropyrazine-2,3-dicarbonitrile (**P3**) as the precursor. This compound underwent treatment with aqueous ammonia in acetonitrile to yield 5,6-diaminopyrazine-2,3-dicarbonitrile (**3**). When compound **3** was reacted with sodium azide in DMSO at 130 °C, the transformation selectively gave 5,6-diamino-3-(1*H*-tetrazol-5-yl)pyrazine-2-carbonitrile (**4**) as the sole product, indicating regioselectivity in the formation of tetrazole. Further modification of compound **4** was achieved by employing a combination of zinc bromide and sodium azide in DMSO at 130 °C which led to the formation of compound **5**. This approach highlights the role of metal-assisted azide activation in directing the structural evolution of the pyrazine core toward functionalized tetrazole derivatives. The diamine derivatives **2** and **5** were further reacted with red fuming nitric acid (100%) in the attempt to make dinitroamine derivatives. Compound **5** upon reaction with nitric acid gave compound **6**, whereas reaction of **2** with nitric acid resulted in the formation of a mixture of compounds. Nitration of compound **2** with various nitrating agents consistently gave complex mixtures and gaseous evolution during workup; no discrete nitration product could be isolated. Literature precedent suggests adjacent amine–tetrazole systems can convert to triazines under nitration, but we found no evidence of an isolable triazine here.

2.2. Characterization

2.2.1. NMR spectroscopy. All the new compounds were analyzed and characterized with ^{1}H, ^{13}C, ^{14}N, and ^{15}N NMR spectroscopy. In the ^{13}C NMR spectrum of **2**, three carbon signals are observed at 155.2, 151.3, and 130.2 ppm (Fig. 2A). For compound **5**, three carbon signals are observed at 153.1, 144.2, and 124.4 ppm (Fig. 2C). After formation of nitroamine, the carbon signals are shifted downfield to 154.0, 148.8,

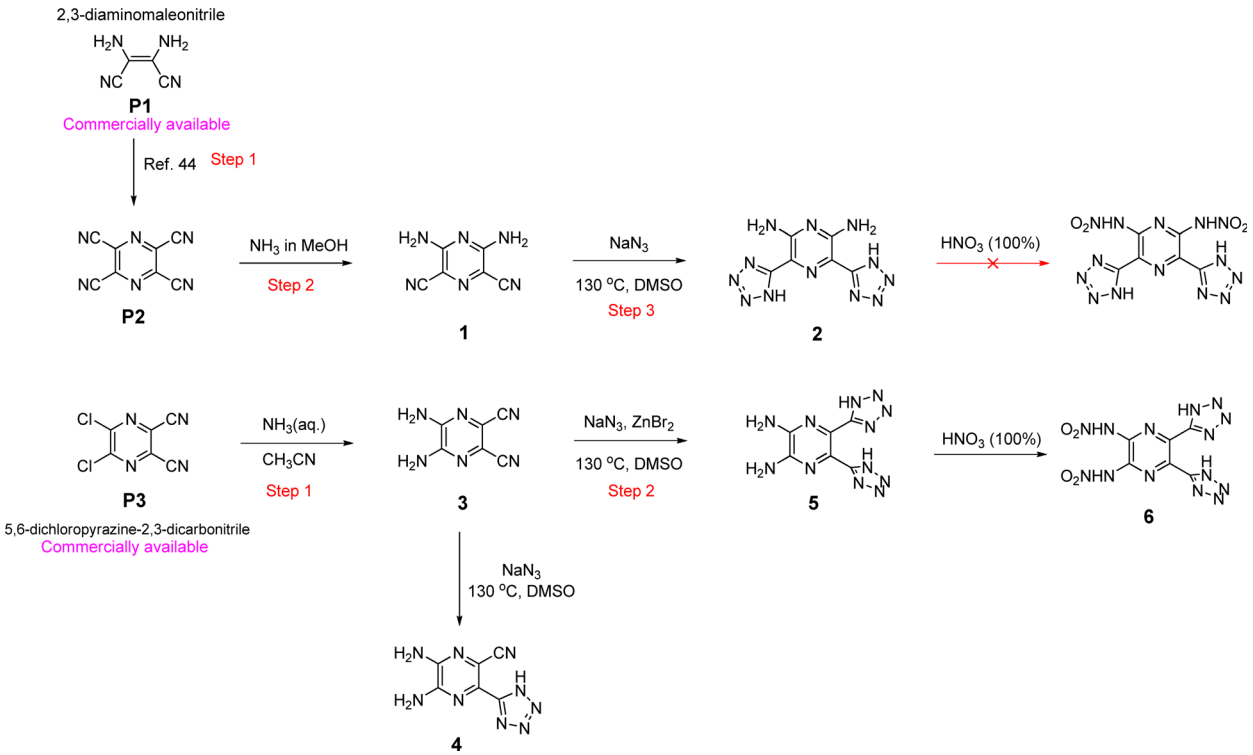

Scheme 1 Synthesis and reactivity of isomeric 3,5-di(1*H*-tetrazol-5-yl)pyrazine-2,6-diamine (**2**) and 5,6-di(1*H*-tetrazol-5-yl)pyrazine-2,3-diamine (**5**).

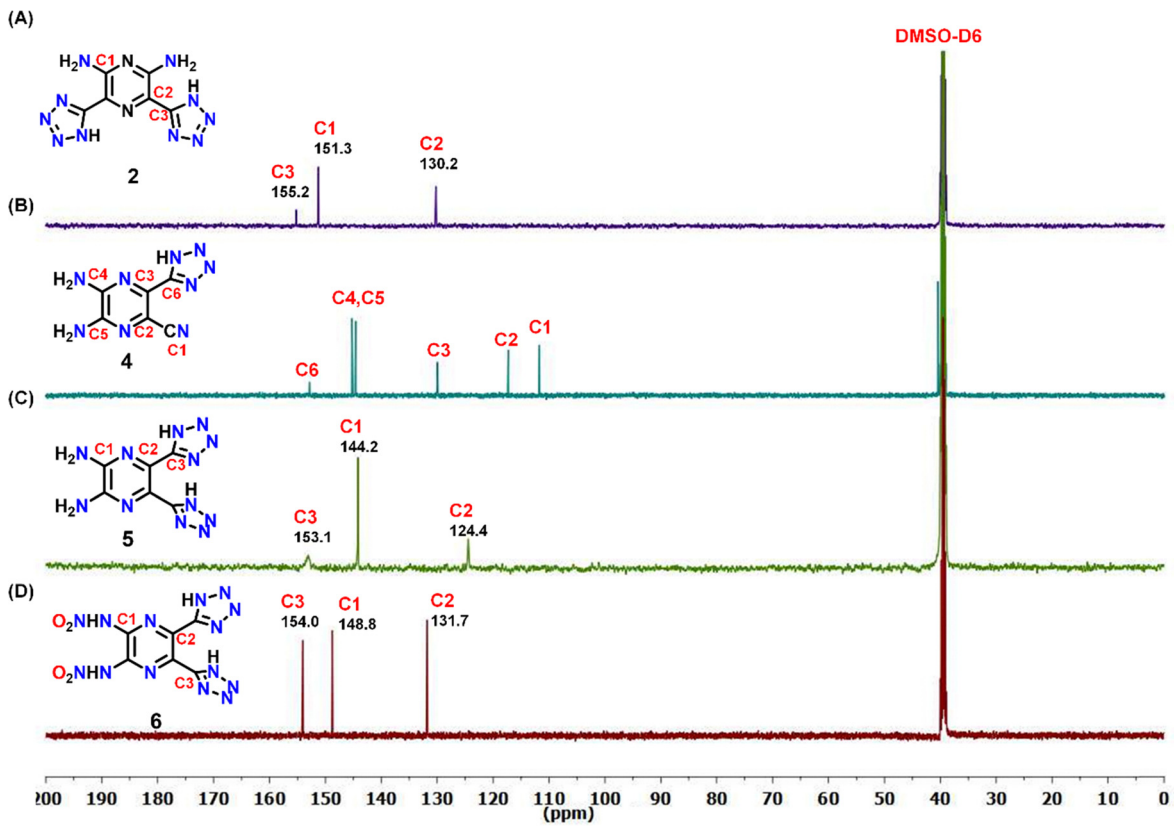

Fig. 2 ^{13}C NMR spectra of (A) **2**. (B) **4**. (C) **5**. (D) **6**.

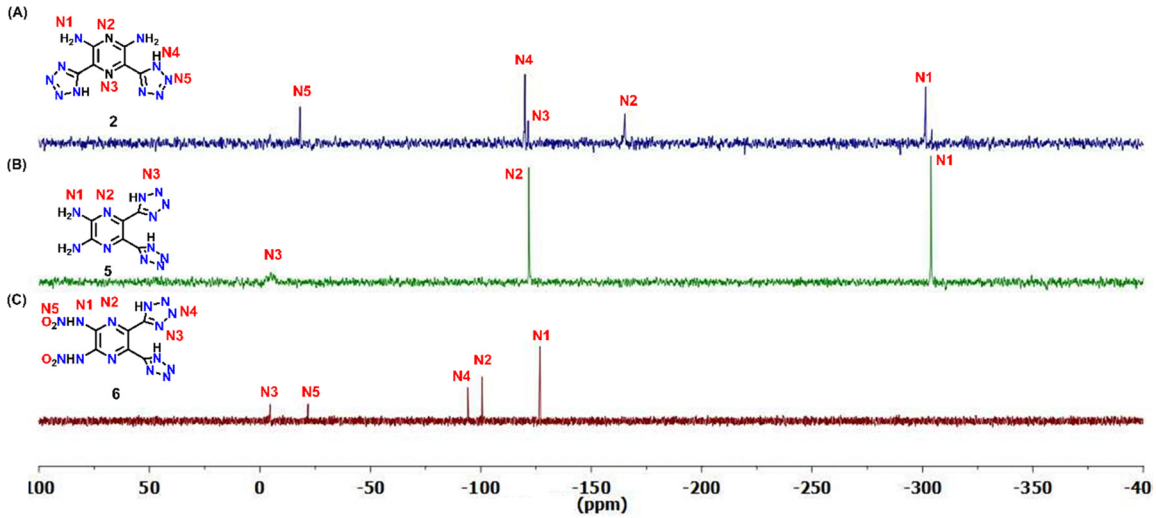

Fig. 3 ^{15}N NMR spectra of (A) **2**. (B) **5**. (C) **6**.

131.7 ppm, respectively (Fig. 2D). In the ^{14}N NMR spectrum of **6**, the nitro group resonance appears at −22.4 ppm. Since all of the compounds are rich in nitrogen, the ^{15}N NMR spectra were recorded and compared. In DMSO-d_6, compound **2** shows five signals at δ −18.09, −120.07, −121.49, −165.18, and −289.97 (Fig. 3A).

The ^{15}N NMR spectrum of the 2,3 isomer **5** has only three signals (Fig. 3B). The tetrazole nitrogen atoms of the two rings shows one broad signal at δ −4.93 (Fig. 3B). The pyrazine nitrogen atoms and amine nitrogen are observed at δ −121.82 and −303.82, respectively. In DMSO-d_6, compound **6** shows five signals at δ −4.55, −21.78, −94.16, −100.57, −126.87 (Fig. 3C). The ^{15}N NMR also confirms the absence of -NH_2 signal and the appearance of $-NO_2$ signal at δ −21.7.

2.2.2. Crystal structure. Compound **2** was isolated as a fine powder. Its characterization was hindered by its poor solubility in water and in common organic solvents including acetone, acetonitrile, and methanol. Single crystals suitable for X-ray diffraction analysis were obtained successfully by slow evaporation from a supersaturated solution of dimethyl sulfoxide (DMSO).

This method allowed for the formation of well-defined crystals necessary for structural determination. Crystallographic analysis showed that compound **2** crystallizes in the triclinic space group $P\bar{1}$, incorporating two DMSO solvent molecules within the crystal lattice (Fig. 4A). At 100 K, the calculated crystal density of compound **2** is 1.509 g cm^{-3}. In the crystal structure, intermolecular and intramolecular hydrogen bonds were observed, with bond lengths ranging from 2.21 to 2.32 Å (Fig. 4C). The π–π interactions arising from molecular stacking were visualized using non-covalent interaction (NCI) plots,[46] and the π–π stacking distances were found to be in the range of 3.25–3.40 Å (Fig. 4D).

2.3. Physiochemical properties

High-energy materials inherently possess a high-energy density, rendering them susceptible to accidental ignition or detonation under thermal stress. Assessing their thermal stability is crucial for determining their safety, as it reflects resistance to unintended decomposition or explosion when exposed to elevated temperatures. To analyze the thermal properties of the newly developed compounds, differential scanning calorimetry (DSC) was employed, providing insight into their decomposition behavior and heat tolerance. Upon heating at 5 °C min^{-1}, the onset of the thermal decomposition of compound **2** occurred at 305 °C. In comparison, compound **5** decomposed at a higher temperature, with an onset at 320 °C. The thermal stabilities of compounds **2** and **5** are higher than that of TNT (295 °C) and comparable to HNS (318 °C).

In addition to their excellent thermal stability, the physicochemical characteristics of compounds **2** and **5** were also examined to assess their environmental and handling stability. Both compounds exhibit extremely low solubility in water and in most common organic solvents such as acetone, acetonitrile, and methanol, consistent with their strong intramolecular interactions (Fig. 4C). Despite their insolubility, both compounds remained stable when suspended in water or exposed to dilute acids for extended periods, showing no visual change or decomposition. The resistance to hydrolysis and degradation highlights the robustness of these pyrazine–tetrazole frameworks and underscores their potential as safe, environmentally stable energetic materials.

The densities of all compounds were measured using a gas pycnometer at ambient temperature in a helium (He) atmosphere and are 1.74 (**2**) and 1.71 (**5**) g cm^{-3}, respectively (Table 1). The enthalpies of formation of the newly synthesized compounds were calculated using the isodesmic method with the Gaussian 03 suite, are 622.9 (**2**) and 648.2 (**5**) kJ mol^{-1} (Table 1).[47] All new compounds have positive enthalpies of formation owing to the presence of multiple N=N bonds. With the measured densities at 25 °C and calculated enthalpies, the detonation properties of **2**, and **5** were calculated using the 7.01.01 version of EXPLO5 to give detonation velocities of 7383

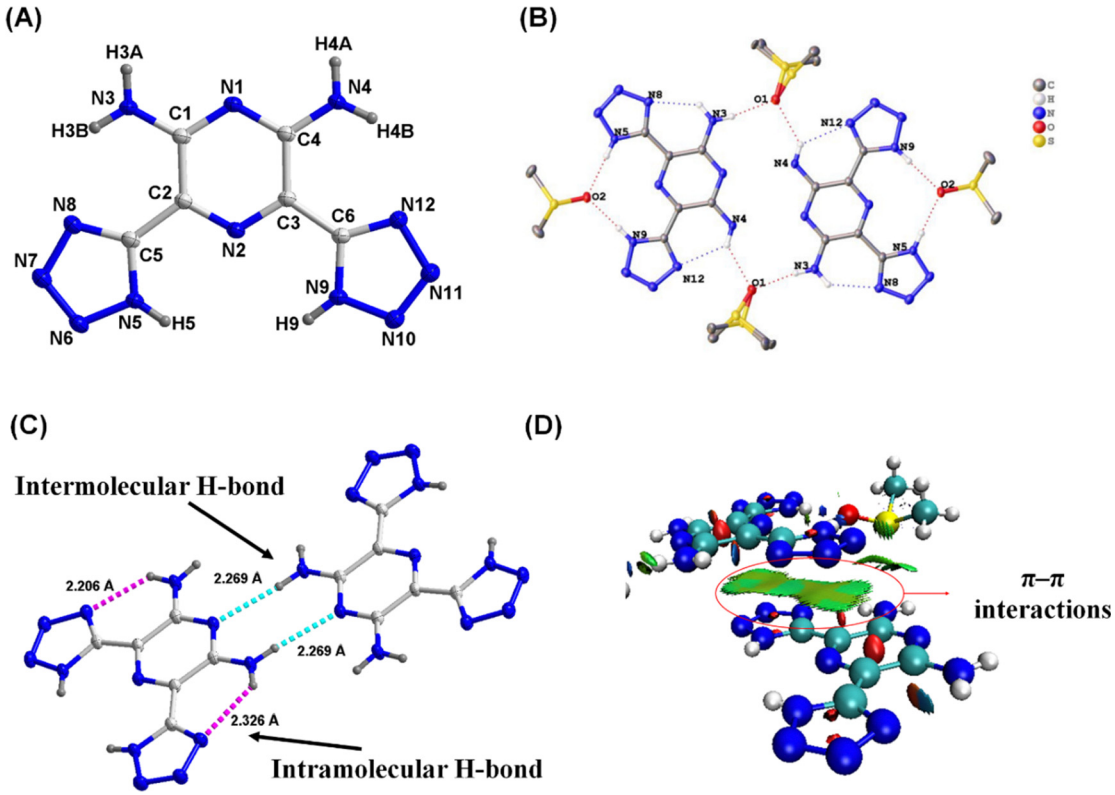

Fig. 4 (A) Labeling scheme for **2•2DMSO** (thermal ellipsoid at 50%). (B) Crystal packing of **2•2DMSO**. (C) Intermolecular and intramolecular bonds. (D) NCIs Plot.

Table 1 Physicochemical properties of compounds

	T_d[a] (°C)	IS[b] (J)	FS[c] (N)	ρ[d] (g cm^{-3})	ΔH_f[e] kJ mol^{-1}	D_v[f] (m s^{-1})	P[g] (GPa)
2	305	40	360	1.74	622.9	7383	18.8
5	320	40	360	1.71	648.2	7278	18.2
HNS	318	5	240	1.74	78.2	7612	24.3
TNT	295	15	353	1.65	−59.4	6824	19.4
RDX	204	7.5/5.6[h]	120	1.80	92.6	8795	34.9

[a] Temperature (onset at 5 °C min^{-1}) of decomposition. [b] Sensitivity to impact (IS). [c] Sensitivity to friction (FS). [d] Density at 25 °C using gas pycnometer. [e] Molar enthalpy of formation (calculated using isodesmic reactions with the Gaussian 03 suite of programs (revision D.01). [f] Velocity. [g] Pressure (calculated using EXPLO5 version 7.01.01). [h] h_{50} = 24 cm/2.5 kg hammer.

(**2**) and 7278 m s^{-1} (**5**), and pressures of 18.8 (**2**) and 18.2 GPa (**5**), respectively. The detonation properties of **2** and **5** surpass those of TNT and approach the performance of HNS, while remaining below the levels exhibited by RDX.

These results suggest that the new compounds are suitable for moderate-performance energetic formulations requiring superior thermal stability and environmental robustness. Upon conversion of the diamine group into a dinitroamine moiety, the compound exhibits a noticeable decrease in thermal stability (212 °C) along with increased sensitivity toward impact and friction (IS = 10 J, FS = 120 N). This behavior can be attributed to the introduction of the electron-withdrawing nitro groups, which weaken the overall molecular framework and enhance sensitivity. Moreover, since the nitramine functionality tends to deviate from the molecular plane, compound **6** does not gain any appreciable advantage in density, resulting in only marginal improvement in overall energetic performance.

3. Conclusions

In this work, we have designed and synthesized new pyrazine-based materials that integrate high nitrogen content, facile synthetic accessibility, and remarkable thermal stability. Structural analysis revealed planar frameworks stabilized by π–π stacking and extensive hydrogen bonding, which contribute to high crystal densities and enhanced robustness. Thermal analyses demonstrated decomposition temperatures that exceed those of conventional pyrazine derivatives and are comparable to benchmark energetic materials. The balance of synthetic simplicity, thermal robustness, and energetic

performance underscores their potential utility as next-generation energetic materials.

Conflicts of interest

The authors declare that they have no competing financial interests or personal relationships that could have influenced the work reported in this paper.

Data availability

The data underlying this study are available in the published article and its online supplementary information (SI). Supplementary information is available. See DOI: **https://doi.org/10.1039/d5ma01131k**.

CCDC 2492520 contains the supplementary crystallographic data for this paper.[48]

Acknowledgements

The diffractometer (Rigaku Synergy S) for SC-XRD was purchased with support from the National Science Foundation (MRI program) under grant no. 1919565. We are grateful to the Fluorine-19 fund for support.

References

1 N. Fischer, D. Fischer, T. M. Klapötke, D. G. Piercey and J. Stierstorfer, *J. Mater. Chem.*, 2012, **22**, 20418.
2 T. M. Klapötke, *High Energy Density Materials*, Springer, Berlin, 2012.
3 J. Li, Y. Liu, W. Ma, T. Fei, C. He and S. Pang, *Nat. Commun.*, 2022, **13**, 5697.
4 H. Gao and J. M. Shreeve, *Chem. Rev.*, 2011, **111**, 7377–7436.
5 N. V. Muravyev, L. Fershtat and Q. Zhang, *Chem. Eng. J.*, 2024, **486**, 150410.
6 L. Hu, P. Yin, G. Zhao, C. He, G. H. Imler, D. A. Parrish, H. Gao and J. M. Shreeve, *J. Am. Chem. Soc.*, 2018, **140**, 15001–15007.
7 M. Benz, T. M. Klapötke and J. Stierstorfer, *Energy Mater. Front.*, 2022, **3**, 161–165.
8 J. Singh, R. J. Staples and J. M. Shreeve, *Sci. Adv.*, 2023, **9**, eadk3754.
9 W. Zhang, Y. Yang, Y. Wang, T. Fei, Y. Wang, C. Sun and S. Pang, *Chem. Eng. J.*, 2023, **451**, 138609.
10 S. Banik, P. Kumar, V. D. Ghule, S. Khanna, D. Allimuthu and S. Dharavath, *J. Mater. Chem. A*, 2022, **10**, 22803–22811.
11 W. Zhang, J. Zhang, M. Deng, X. Qi, F. Nie and Q. Zhang, *Nat. Commun.*, 2017, **8**, 181.
12 B. Tan, J. Su, J. Zhang, C. Tang, J. Dou, X. Yang, M. Xu, S. Zeng, W. Li, J. Luan, G. Zhang, S. Song, Q. Zhang, X. Lu, B. Wang and N. Liu, *J. Mater. Chem. A*, 2025, **13**, 25103–25109.
13 X. Guo, Y. Feng, Y. Liu, Q. Liu, L. Q. Luo and H. Gao, *J. Mater. Chem. A*, 2025, **13**, 10782–10791.
14 Y. Shan, S. Huang, T. Jiang, Y. Cao, J. Wang, Y. Cao and W. Zhang, *J. Mater. Chem. A*, 2025, **13**, 1164–1171.
15 C. Li, T. Zhu, C. Wang, L. Chen, C. Lei, J. Tang, H. Yang, C. Xiao and G. Cheng, *J. Mater. Chem. A*, 2024, **12**, 24188–24194.
16 X. Cui, T. Yu, H. Xia, J. Wu, J. Wei, X. Qi and H. Wei, *J. Mater. Chem. A*, 2025, **13**, 28874–28879.
17 J. Singh, R. J. Staples and J. M. Shreeve, *J. Mater. Chem. A*, 2023, **11**, 12896–12901.
18 K. Pandey, A. Tiwari, J. Singh, P. Bhatia, P. Das, D. Kumar and J. M. Shreeve, *Org. Lett.*, 2024, **26**, 1952–1958.
19 J. Singh, R. J. Staples and J. M. Shreeve, *J. Mater. Chem. A*, 2024, **12**, 30548–30557.
20 C. Li, S. Wang, S. Li, H. Yin, Q. Ma and F. X. Chen, *ACS Appl. Mater. Interfaces*, 2024, **16**, 35232–35244.
21 D. Kumar and A. J. Elias, *Resonance*, 2019, **24**, 1253–1271.
22 M. Benz, T. M. Klapötke, J. Stierstorfer and M. Voggenreiter, *J. Am. Chem. Soc.*, 2022, **144**, 6143–6147.
23 A. J. Bennett, L. M. Foroughi and A. J. Matzger, *J. Am. Chem. Soc.*, 2024, **146**, 1771–1775.
24 Q. Yu, Z. Zheng, Z. Yi, W. Yi and J. M. Shreeve, *J. Am. Chem. Soc.*, 2025, **147**, 5125–5131.
25 X. Jiang, D. Yin, S. Song, Y. Wang, M. Fan, R. Wang and Q. Zhang, *J. Mater. Chem. A*, 2024, **12**, 13231–13239.
26 S. Chen, L. Li, S. Song and Q. Zhang, *Cryst. Growth Des.*, 2023, **23**, 4970–4978.
27 W. Huang, Y. Tang, G. H. Imler, D. A. Parrish and J. M. Shreeve, *J. Am. Chem. Soc.*, 2020, **142**, 3652–3657.
28 Y. Hu, W. S. Dong, Z. J. Lu, H. Zhang and J. G. Zhang, *Chem. Commun.*, 2023, **59**, 9864–9867.
29 R. Lu, N. Du, S. Jiang, M. Lu and P. Wang, *Cryst. Growth Des.*, 2025, **25**, 4304–4315.
30 R. Rajak, P. Kumar and S. Dharavath, *Cryst. Growth Des.*, 2024, **24**, 2142–2148.
31 J. Wang, R. Lv, S. Song, L. Wei, S. Huang, Q. Zhang and K. Wang, *Cryst. Growth Des.*, 2024, **24**, 4114–4121.
32 J. Zhang, Q. Zhang, T. T. Vo, D. A. Parrish and J. M. Shreeve, *J. Am. Chem. Soc.*, 2015, **137**, 1697–1704.
33 R. Zhang, Y. Xu, F. Yang, S. Jiang, P. Wang, Q. Lin, H. Huang and M. Lu, *J. Org. Chem.*, 2024, **89**, 5966–5976.
34 X. Jiang, M. Fan, R. Wang, Y. Wang and Q. Zhang, *Chem. Commun.*, 2025, **61**, 9924–9927.
35 X. Zhang, L. Pan, M. Li, J. Jing, H. Xia and Q. Zhang, *CrystEngComm*, 2025, **27**, 5021–5029.
36 J. Cai, C. Xie, J. Xiong, J. Zhang, P. Yin and S. Pang, *Chem. Eng. J.*, 2022, **433**, 134480.
37 G. Zhang, H. Xiong, P. Yang, C. Lei, W. Hu, G. Cheng and H. Yang, *Chem. Eng. J.*, 2021, **404**, 126514.
38 Q.-N. Tariq, M.-U.-N. Tariq, S. Manzoor, Q. Yu and J.-G. Zhang, *Dalton Trans.*, 2025, **54**, 12454–12462.
39 Y. Wang, J. Liu, J. He, X. Ren, L. Hu and S. Pang, *Chem. Commun.*, 2025, **61**, 13433–13436.
40 T. M. Klapötke and T. G. Witkowski, *ChemPlusChem*, 2016, **81**, 357–360.
41 J. Singh, A. K. Chinnam, R. J. Staples and J. M. Shreeve, *Inorg. Chem.*, 2022, **61**, 16493–16500.

42 A. K. Yadav, V. D. Ghule and S. Dharavath, *Chem. – An Asian J.*, 2024, **19**, e202400409.
43 P. Pagoria, M. Zhang, N. Zuckerman, G. Lee, A. Mitchell, A. DeHope, A. Gash, C. Coon and P. Gallagher, *Propellants, Explos., Pyrotech.*, 2018, **43**, 15–27.
44 T. G. Witkowski, E. Sebastiao, B. Gabidullin, A. Hu, F. Zhang and M. Murugesu, *ACS Appl. Energy Mater.*, 2018, **1**, 589–593.
45 T. G. Witkowski, P. Richardson, B. Gabidullin, A. Hu and M. Murugesu, *ChemPlusChem*, 2018, **83**, 984–990.
46 T. Lu and F. Chen, *J. Comput. Chem.*, 2012, **33**, 580–592.
47 M. J. Frisch, G. W. Trucks, H. B. Schlegel, G. E. Scuseria, M. A. Robb, J. R. Cheeseman, G. Scalmani, V. Barone, B. Mennucci, G. A. Petersson, H. Nakatsuji, M. L. Caricato, X. Li, H. P. Hratchian, A. F. Izmaylov, J. Bloino, G. Zheng, J. L. Sonnenberg, M. Hada, M. Ehara, K. Toyota, R. Fukuda, J. Hasegawa, M. Ishida, T. Nakajima, Y. Honda, O. Kitao, H. Nakai, T. Vreven, J. A. MontgomeryJr, J. E. Peralta, F. Ogliaro, M. Bearpark, J. J. Heyd, E. Brothers, K. N. Kudin, V. N. Staroverov, R. Kobayashi, J. Normand, K. Raghavachari, A. Rendell, J. C. Burant, S. S. Iyengar, J. Tomasi, M. Cossi, N. Rega, N. J. Millam, M. Klene, J. E. Knox, J. B. Cross, V. Bakken, C. Adamo, J. Jaramillo, R. Gomperts, R. E. Stratmann, O. Yazyev, A. J. Austin, R. Cammi, C. Pomelli, J. W. Ochterski, R. L. Martin, K. Morokuma, V. G. Zakrzewski, G. A. Voth, P. Salvador, J. J. Dannenberg, S. Dapprich, A. D. Daniels, Ö. Farkas, J. B. Foresman, J. V. Ortiz, J. Cioslowski and D. J. Fox, *Revision D.01*, Gaussian, Inc, Wallingford, CT, 2003.
48 CCDC 2492520: Experimental Crystal Structure Determination, 2025, DOI: **10.5517/ccdc.csd.cc2pnnwx**.